

# Effect of process parameters on electromagnetic impact welding of aluminum sheets

S.D. Kore<sup>a</sup>, P.P. Date<sup>a,\*</sup>, S.V. Kulkarni<sup>b</sup>

<sup>a</sup>Mechanical Engineering Department, IIT Bombay, Powai, Mumbai 400076, Maharashtra, India

<sup>b</sup>Electrical Engineering Department, IIT Bombay, Powai, Mumbai 400076, Maharashtra, India

Received 11 April 2006; received in revised form 24 August 2006; accepted 29 August 2006

Available online 16 November 2006

---

## Abstract

Electromagnetic forming of aluminum sheets has been studied in detail by many researchers due to its advantages of increased formability and reduced springback. The feasibility of electromagnetic impact welding of aluminum sheets has been established, but the effect of process parameters on the weld strength has not been reported. The present study investigates the effect of parameters such as energy, standoff distance and coil geometry on the shearing strength and the width of the weld achieved by electromagnetic impact welding of aluminum sheets. A study has been carried out to characterize the effectiveness of the process of welding two aluminum sheets of same chemical composition and of 1 mm thickness. The results of the microstructure and shearing strength tests are reported in this paper. The shearing strength and the width of the weld are found to increase with an increase in discharge energy. Further, when the geometry of the coil is changed from rectangular shape to tapered shape, it gives higher shearing strength. The standoff distance has an optimum value that gives maximum shearing strength and width of the weld. If the standoff distance is varied on either side of its optimum value the shearing strength and the width of the weld reduce.

© 2006 Elsevier Ltd. All rights reserved.

*Keywords:* Electromagnetic; Welding; Shearing strength; Microstructures; Process parameters

---

## 1. Introduction

Electromagnetic (EM) forming is a technique for forming of metals by means of plastic deformation generated by a repulsive force on account of the interaction between magnetic field of coil and current induced in workpiece. A primary high strength transient magnetic field is produced when capacitive stored energy is discharged into an inductor. An opposing magnetic field is generated from the eddy currents induced in the metallic work piece [1]. The impact velocity of the work piece is more than 300 m/s and, therefore, this process is also called as high-velocity forming process [2].

Aluminum (Al) and magnesium (Mg) are engineering materials that have high electrical conductivity, low melting point, high vapor pressure, high affinity for oxygen and low-yield strength. Application of heat often

---

\*Corresponding author. Tel.: +91 22 25767511; fax: +91 22 25726875.

E-mail address: [ppdate@iitb.ac.in](mailto:ppdate@iitb.ac.in) (P.P. Date).

leads to serious weld defects, and hence they are appropriate work materials for electromagnetic forming (EMF) [3]. Aluminum, being a light weight material, has wide applications in automobile and aerospace industries. However, formability and weldability still remain major issues for aluminum. Nevertheless, while forming aluminum alloys using high-energy rate forming methods, the formability of aluminum can be significantly increased [4]. Being a high strain rate forming method, the EMF process has all the advantages of high-velocity forming process; viz. increased formability, reduced springback and reduced wrinkling of formed parts [5,6]. The EM forming process for flat sheets and axi-symmetric components (tubes) has been studied in detail by many researchers [7,8]. Due to the ease in controlling the magnetic field enveloped inside the tubes the electromagnetic technique has been widely used for tube welding [9,10]. This has been further investigated in detail for characterizing the EM welding technique for welding of similar and dissimilar metal tubes [11–18]. In case of flat components, control of the magnetic field is difficult. Hence, the application of the EM technique gets restricted. The research on electromagnetic impact welding of flat sheets has not been extensively documented and the literature prominently shows the activity of only one researcher in this field [19,20]. No literature reporting characterization of effects of process parameters was found and in that sense, this paper attempts to make a novel contribution to the existing literature on the subject. The present work investigates the effect of process parameters such as energy, standoff distance and coil geometry on the shearing strength and the width of the weld obtained by electromagnetic impact welding of 1 mm flat aluminum sheets.

## 2. Electromagnetic impact welding technique

### 2.1. Bonding mechanism

Welding requires two atomically clean surfaces to be pressed together to obtain metallurgical continuity. This continuity in Al-based alloys is interrupted by  $\text{Al}_2\text{O}_3$ , adsorbed gases and surface contamination. These are however removed during the well-known process of ‘Jetting’ in which due to high-velocity impact the surfaces of two impacting sheets become atomically clean at the time of collision. As the two sheets come together leading to atomically clean surfaces coming together the requirement of weld formation is satisfied and a weld is formed at the interface establishing the metallurgical continuity. This is also borne out by the fact that the boundaries of the two surfaces are not discernible wherever weld has taken place.

### 2.2. Principle of electromagnetic impact welding

Electromagnetic impact welding is based on Ampere’s observation that the force between two infinitely long parallel conductors carrying currents  $I_1$  and  $I_2$  and separated from each other by distance  $d$  may be written as [21]

$$F = \frac{\mu_0}{2\pi d} I_1 I_2 \quad \text{N/m.} \quad (1)$$

It is repulsive when the currents are in opposite direction, and attractive otherwise. For instance, if  $I_1 = I_2 = 1 \text{ A}$ , and  $d = 1 \text{ m}$ , then  $F = 2 \times 10^{-7} \text{ N/m}$ .

The schematic representation of the electromagnetic equipment used for the experimental work is shown in Fig. 1. The electromagnetic impact welding setup consists of capacitor bank, high-voltage charging power supply, work coils, discharge circuit, spark gap (high-voltage switch) and current shunt ( $R$ ).

The photograph of the electromagnetic impact welding facility used for the experimental work is shown in Fig. 2. The energy stored in the capacitor bank, charged through a DC power supply, is discharged through the work coil by triggering the spark gap. The damped sinusoidal current set up in the work coil produces a transient magnetic field. The work sheets in the vicinity of the work coil cut the transient magnetic field. Hence, the induced electromotive force and the corresponding eddy currents in the work sheets oppose their cause. Fig. 3 shows the transient magnetic flux generated by the coil, which induces the eddy currents within the thickness of the sheets. The induced eddy currents depend upon the material properties (conductivity and permeability). Finally, the work sheets are repelled away from the coil (towards each other) creating an

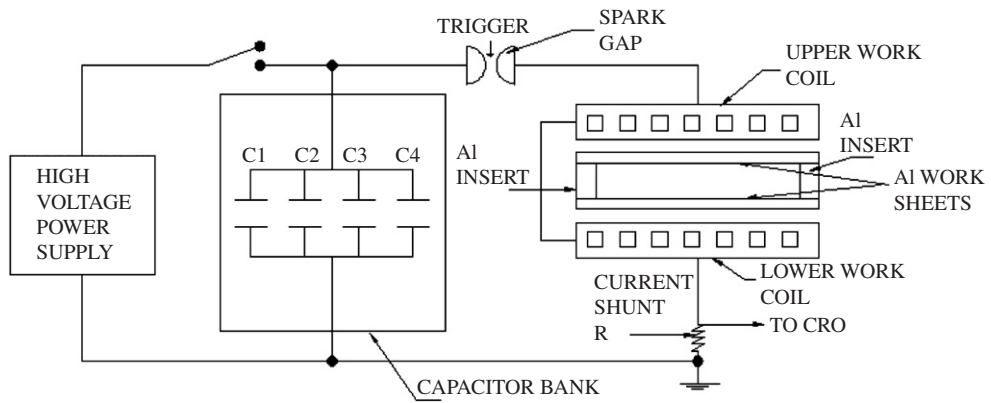


Fig. 1. Schematic representation of electromagnetic impact welding equipment.



Fig. 2. Experimental setup for electromagnetic impact welding.

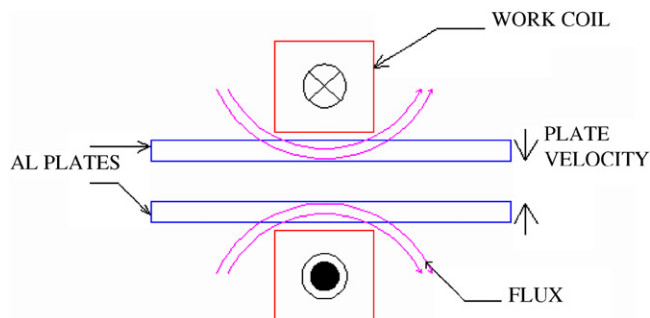


Fig. 3. Magnetic flux and induced eddy current.

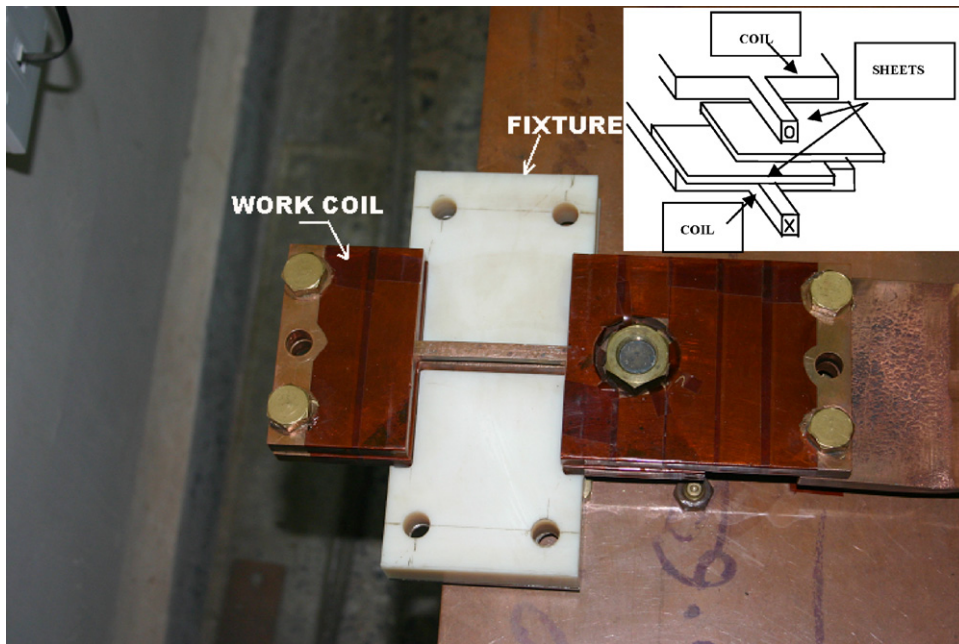


Fig. 4. Photograph of three-dimensional flat rectangular coil for EM welding.

impact, due to Lorentz force, which lasts for a few microseconds, on account of the interaction between the induced eddy currents and the magnetic field. The ‘Jetting’ due to high-velocity impact, causes the expulsion of the oxides on the surface and clears the colliding work sheet surfaces. After the collision, the atomically clean work sheet surfaces are brought in contact by pressing them together by electromagnetic pressure. The weld is formed at the interface establishing the metallurgical continuity. The energy of the impact and hence the occurrence of the weld depends on parameters such as inductance of the circuit, frequency, capacitor bank energy, voltage, current, and standoff distance between the sheets. The standoff distance is the distance by which the sheets to be welded are separated from each other prior to discharge.

### 2.3. Flat rectangular coil for electromagnetic impact welding

A three-dimensional flat rectangular one turn copper coil as shown in Fig. 4 is designed for the electromagnetic impact welding of 1 mm thick flat aluminum sheets. The web of ‘I’-shaped cross-section of the coil is placed at the center for concentrating the current, thereby increasing the current density  $J$  [19]. An increase in the current density gives a corresponding increase in the resultant Lorentz force that generates high impact between the sheets to be welded. The Lorentz force is given by

$$F = J \times B \quad (2)$$

where  $B$  is magnetic flux generated by the coil in Tesla [21].

### 3. Experimental procedure for electromagnetic impact welding of al sheets

The aluminum sheets of the size 70 mm long, 70 mm wide and 1 mm thick are used in an as-received condition and cleaned with acetone. Special surface preparation is not necessary for carrying out the electromagnetic impact welding of Al sheets, since the surface oxides are removed during the phase of jet formation that precedes the phase of bond formation. The two aluminum work sheets, to be welded are kept within the work coil. The ends of the sheets are connected electrically with the help of Al inserts as shown in Fig. 1 to facilitate the flow of eddy currents through the sheets and avoid arcing between them. The properties of the aluminum material used are summarized in Table 1.

Table 1  
Properties of Al alloy used for electromagnetic impact welding

Alloy designation and temper	Density (kg/mm <sup>3</sup> )	Electrical resistivity ohm-cm	Yield strength (YS) (MPa)	UTS (ultimate tensile strength) (MPa)
Aluminum 1050-O	2700	$2.81 \times 10^{-6}$	28	76

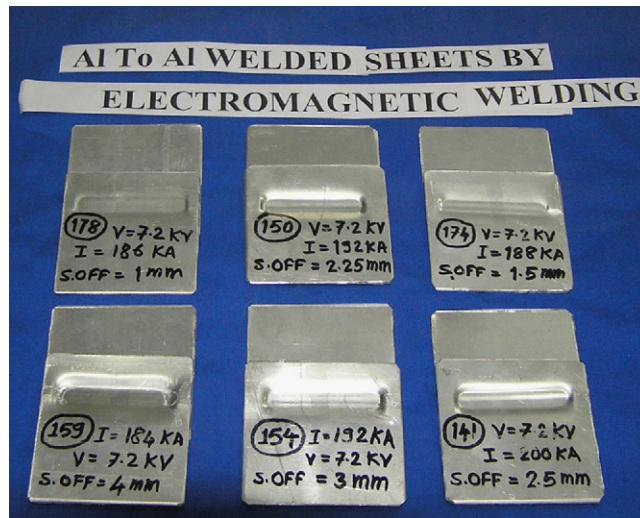


Fig. 5. Al to Al EM welded samples.

Fig. 5 shows the photograph of six representative samples of the total of 75 samples of Al sheets welded at six different standoff distances while the energy was kept constant. The bank capacity used for all the experiments was 10 kJ at 10 kV. Copper coil having inductance of 0.74 nH was used. The web of 5 mm wide and 70 mm long, having 'I'-shaped cross-section, was placed at the center to increase the current density. The total inductance of the circuit was 0.7  $\mu$ H. The web of the 'I'-shaped section of the coil was supported with a specially designed and fabricated nested-type nylon fixture, as shown in Fig. 4, to avoid its bending in the process of welding of the sheets.

The experimental parameters were adjusted such as to have ringing frequency of 18.50 kHz and ensure that the skin depth of the job piece was less than its thickness. Under this condition an appreciable amount of magnetic field was confined within the thickness of sheets and the diffusion of the field through the sheets was reduced to a minimum value. The skin depth is given by [1]

$$\delta = \frac{1}{\sqrt{(\pi\sigma\mu f)}}, \quad (3)$$

where  $\delta$  is the skin depth, m;  $\mu$  the permeability of the job piece, H/m; and  $f$  the ringing frequency of transient current, Hz.

If the skin depth thickness is one-third of the sheet thickness or less, the magnetic field does not diffuse out of the job piece [3]. Based on the experimental parameters set, the maximum value of the first peak of current was 202 kA. The current value is measured using the CRO, which gets the input from the current shunt ( $R$ ) connected in the circuit as shown in Fig. 1. The damped sinusoidal oscillating current waveform is shown in Fig. 6, which was obtained with an energy storage capacitor having specifications of 10 kJ and 20 kV, when voltage and energy values were set to 7.2 kV and 5 kJ, respectively.

The values of  $d_1$  and  $d_2$  in Eq. (4) were determined for the initial position of the sheets with respect to the coil, i.e., position of sheets before collision. The values of  $d_1$  and  $d_2$ , determined using the final position of the sheets with respect to the coils, i.e., at the time of collision, are also given below. The magnetic flux density was

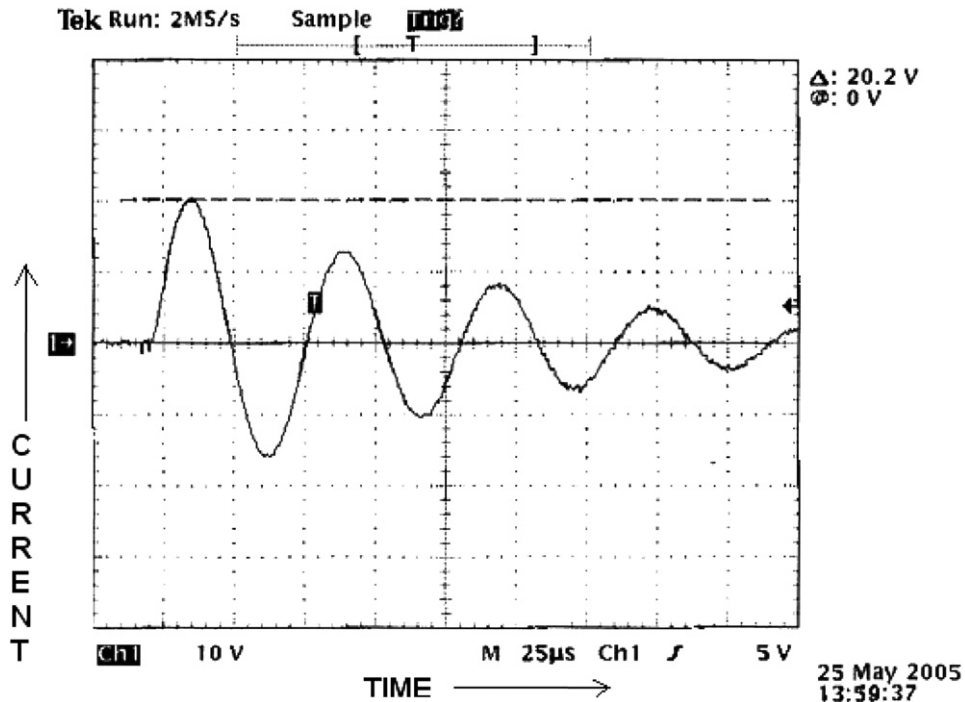


Fig. 6. Current waveform at 5 kJ discharge energy, standoff distance = 2.5 mm, 100 kA/div and 25  $\mu$ S/div.

determined as [19]

$$B = \mu I \frac{[\tan^{-1}(b/2d_1) + \tan^{-1}(b/2d_2)]}{\pi b}, \quad (4)$$

where  $I$  is the discharge current, A;  $b$  the width of the middle 'T'-shaped web portions of the coil, m;  $d_1, d_2$  the distances of the sheets from the inner surfaces of the upper and lower 'T'-shaped web of the coil, respectively, m.

At initial position of the sheet,  $d_1 = d_2 = 0.07 \times 10^{-3}$  m.

At final position of the sheet,  $d_1 = d_2 = 1.5 \times 10^{-3}$  m.

The maximum magnetic flux density reduces from its initial value of 50 T to average value of 33 T at the time of collision. This corresponds to an initial pressure of 950 MPa and a collision pressure of 425 MPa as per Eq. (5) [19]:

$$P = \frac{B^2}{2\mu} [1 - \exp(-2t/\delta)], \quad (5)$$

where  $P$  is the magnetic pressure, Pa;  $t$  the thickness of the sheet, m.

#### 4. Effect of process parameters on the strength and the width of the weld

A study was carried out to investigate the effect of the process parameters, viz. coil geometry, energy and standoff distance. Experiments were carried out to study the effect of the variation in energy and standoff distance for two geometries of coils, one with a rectangular area of cross-section and the other with a tapered cross-section (Fig. 7). The samples welded using either of the coils were laser-cut in to three pieces A, B, and C, as shown in Fig. 8 and tested for shearing strength of the weld. Shearing strength of the lap weld obtained by EM welding is determined by uni-axial tensile test and calculated using Eq. (6).

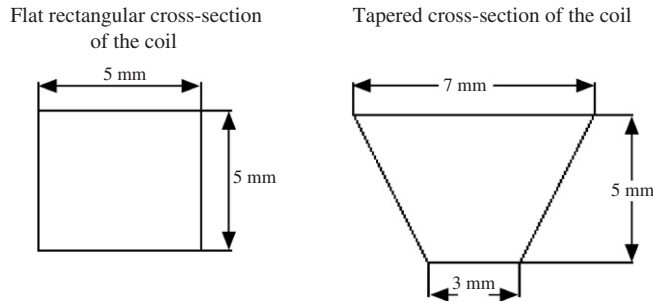


Fig. 7. Cross sections of the coils.

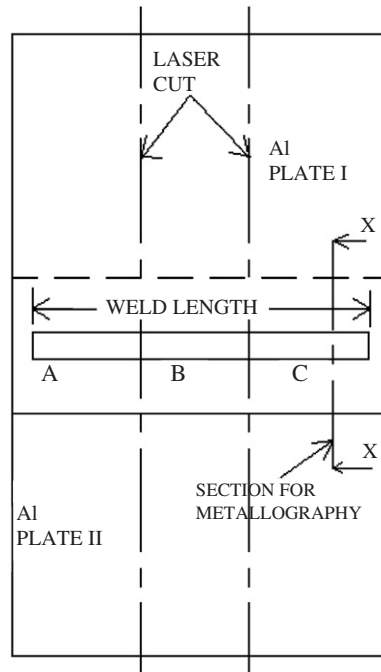


Fig. 8. Laser cut pieces from the electromagnetically welded samples.

Shearing strength of the weld or

$$(\text{Stress in uniaxial tension; } \sigma_y) = \frac{\text{Axial load in tensile test at failure}}{\text{Area of the lap welded joint } (A_l)}, \tag{6}$$

$$\tau = \frac{\text{UTS} \times A_0}{A_l}, \tag{7}$$

$$k = \frac{\sigma_y}{\sqrt{3}}, \tag{8}$$

where  $\tau$  is the shear stress,  $A_0$  the area of cross-section of the Al sheet,  $\sigma_y$  the stress in uniaxial tension and  $k$  the yield strength under shear:

If  $\tau/k \geq 1$ , then sample failed in the weld,

If  $\tau/k \leq 1$  then sample failed in the parent metal.

When the yield strength under shear ( $k$ ) is greater than the shear stress ( $\tau$ ) the sample fails in the parent metal giving the weld stronger than the parent metal. Some of the samples tested for uni-axial tensile test satisfy the condition  $\tau/k \leq 1$  and failed in the parent metal as shown in Fig. 9. This indicates that welds

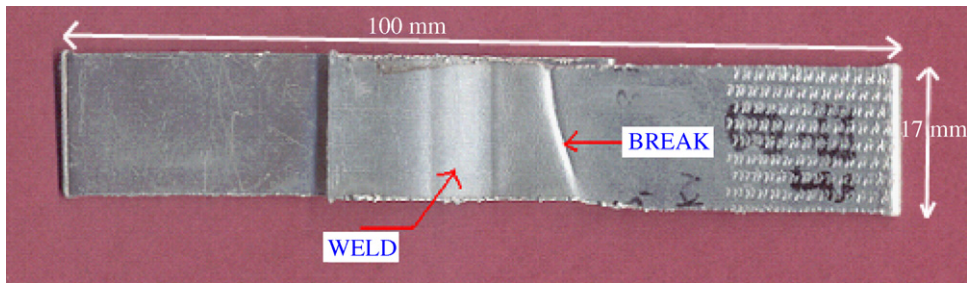


Fig. 9. Specimen for uni-axial tensile test showing break in the parent metal.

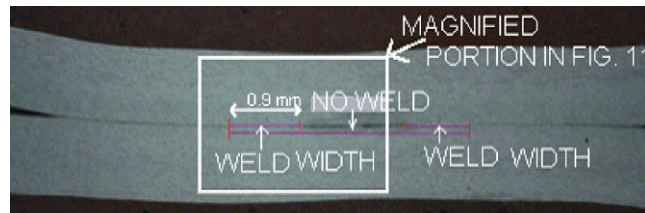


Fig. 10. Al to Al electromagnetically welded sample showing weld and no-weld zones.

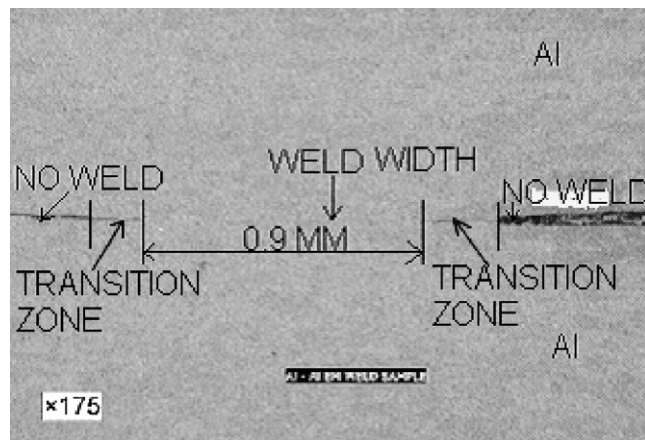


Fig. 11. Magnified view of the weld zone indicated in Fig. 10.

obtained are stronger than the parent metal, a desirable result. The samples which failed in the parent metal are indicated with the unfilled data points ( $\diamond$   $\square$   $\triangle$ ) whereas, those failed in the weld are indicated with the filled data points ( $\blacklozenge$   $\blacksquare$   $\blacktriangle$ ) in the graphs shown in Figs. 14 and 17.

The welded samples were subsequently sectioned across the weld (section X–X shown in Fig. 8), metallographically polished, and etched to determine the zone of actual metallurgical continuity. The effect of process parameters on the weld width could then be established. The metallographic study of the Al–Al welded samples shows the weld and no-weld zones (Fig. 10). Two weld zones and one no-weld zone at the center are clearly seen. Further magnification of the weld zone is shown in Fig. 11. The weld zone shows the total metallurgical continuity of the metals. The transition zone between weld and no-weld zone has wavy interface as the physical boundaries of the two sheets are retained. The reasons for the no-weld zone at the center are:

1. At the time of collision the Lorentz forces acting on the Al sheets are normal to the sheet at the center and it has shear component elsewhere as shown in Fig. 12. Hence, Al sheets collide with each other at the center

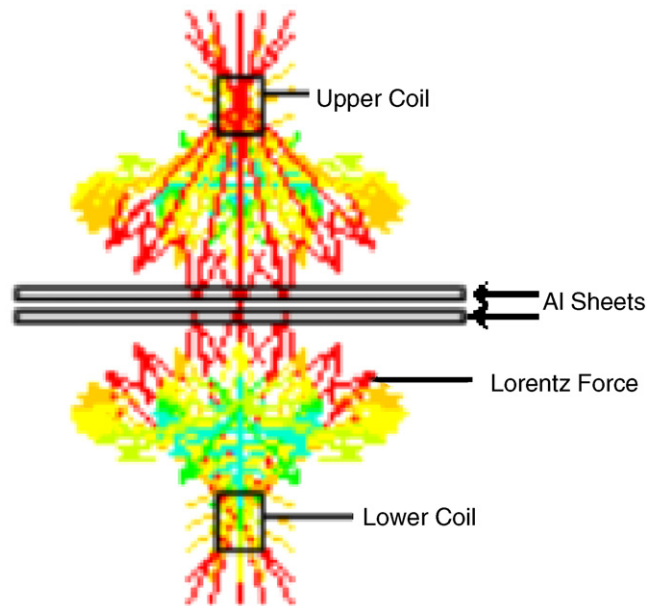


Fig. 12. Lorentz forces acting on the sheets at the time of collision. Force in the center is normal to the sheet while it has a shear component elsewhere.

and this gives rebound effect leading to no-weld zone at the center. As there is no rebound effect away from the center, the colliding sheets remain in contact with each other leading to weld zones.

2. Entrapment of oxide on the colliding surfaces of the Al sheets at the center because the two sheets are placed parallel to each other, unlike the case where an angular placement of the sheets enables expulsion of the oxides effectively.
3. The other possible reason that may be contributing is complex deformation state at the interface. This need to be further investigated.

The percentage weld width is determined by using Eq. (9) for each weld to analyze the effect of process parameters on it:

$$\% \text{Weld width} = \frac{\text{Total width of the weld}}{\text{Width of the web cross section of the coil}} \times 100. \quad (9)$$

#### 4.1. Effect of coil geometry on the weld strength and width

The effect was investigated for two types of coil cross-section, viz. rectangular and tapered (Fig. 7).

##### 4.1.1. Weld strength

Reduced cross-sectional area of tapered coil leads to an increase in the current density at the 'I' section, magnetic flux density, and the Lorentz force. Hence the tapered coil would be expected to give a stronger weld as compared to the rectangular coil. The results of the shearing strength test (discussed in Sections 4.2.1 and 4.3.1) show the superiority of the tapered coil geometry in increasing the shearing strength of the weld. The weld strength obtained with the flat coil is 75 MPa at values of discharge energy and standoff distance set to 5 kJ and 2.5 mm, respectively, whereas, that obtained with the same set of the process parameters with the tapered coil is in excess of 96 MPa.

4.1.2. Weld width

With the coil having rectangular cross-section it was not possible to vary the current density and the weld area since the two opposite faces of the coil had same dimensions. Tapered cross-section of the coil facilitates two different values of current density and the weld areas. The comparison of the percentage weld widths obtained with the tapered and rectangular coils when the energy and standoff distances are varied is shown in Figs. 13(a) and (b). The removal rate of oxides entrapped on the colliding surfaces of the Al sheets at the smaller values of standoff distance and energy is lesser whereas, for the higher values it is greater. For lower values of energy and standoff distance, the percentage weld widths obtained with the tapered coil are smaller as compared with those obtained with the flat rectangular coil. On the contrary, for larger values of the standoff distances and energy the percentage weld widths obtained with the tapered coil are larger than those obtained with the rectangular coil. The reason for a reduced percentage weld width with the tapered coil as compared with the rectangular coil is a smaller spread of magnetic field due to a reduced cross-section of the tapered coil. It reduces the portion of the Al sheet in which the magnetic field is penetrated and the eddy currents are induced.

4.2. Effect of energy on the weld strength and width

Investigation of the effect of energy on the shearing strength of the weld was carried out by welding aluminum sheets with energy ranging from 3.6 to 5 kJ (obtained by varying the capacitor charging voltage), while the values of bank capacitance and the standoff distance being kept constant at 200 μF and 2.5 mm, respectively.

4.2.1. Weld strength

4.2.1.1. Flat rectangular coil. The dependency of the shearing strength on the energy for flat rectangular coil is shown in Fig. 14(a). Increase in energy enhanced the shearing strength of the welds. The ‘B’ pieces cut from the central part of all the welds show higher shearing strength as compared to the ‘A’ and ‘C’ pieces cut from the edges of the welded samples. The reason for the greater shearing strength at the center is high penetration of magnetic field at the center than at the edges and that the current flowing through sheets changed direction at the edges. This weakens the magnetic field developed at the edges and hence the pressure acting on the sheets. The shearing strength of the weld obtained is 75 MPa with the discharge energy of 5 kJ whereas, the value is 29 MPa at 3.6 kJ discharge energy.

4.2.1.2. Tapered coil. Fig. 14(b) shows the graph of energy versus shearing strength of the welds obtained with the coil having the tapered cross-sectional area. Increase in energy for the welding has enhanced the shearing strength of the welds. Similar to the rectangular coil, the ‘B’ test pieces have higher shearing strength than the ‘A’ and ‘C’ pieces. The value of the shearing strength obtained is in excess of 96 MPa (28% higher

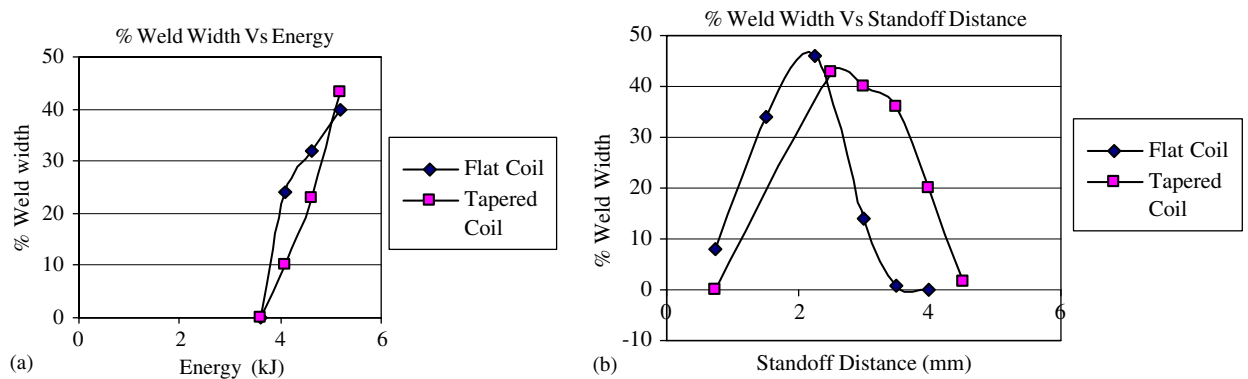


Fig. 13. (a) Comparison of the % weld widths obtained at standoff distance = 2.5 mm, (b) Comparison of the % weld widths obtained at discharge energy = 5 kJ.

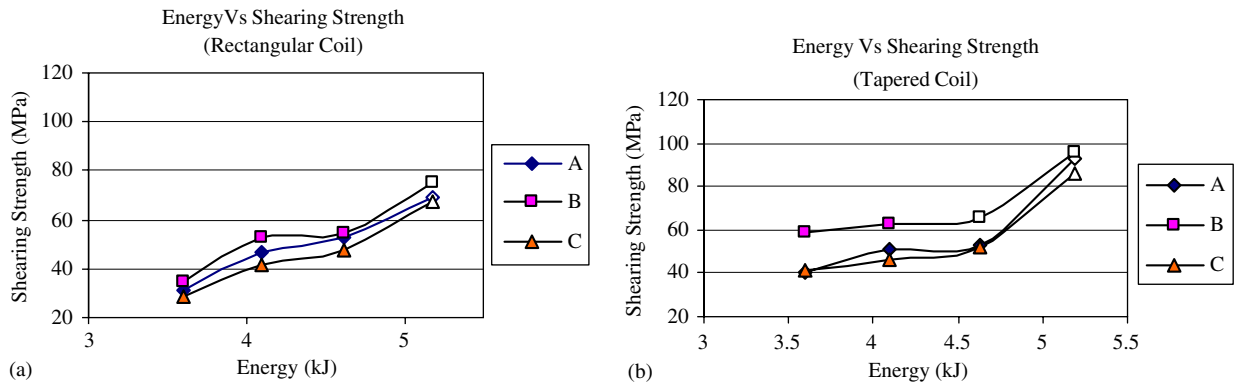


Fig. 14. (a) Rectangular coil: effect of energy on the shear strength of the weld, with standoff distance = 2.5 mm, (b) tapered coil: effect of energy on the shear strength of the weld with standoff distance = 2.5 mm.

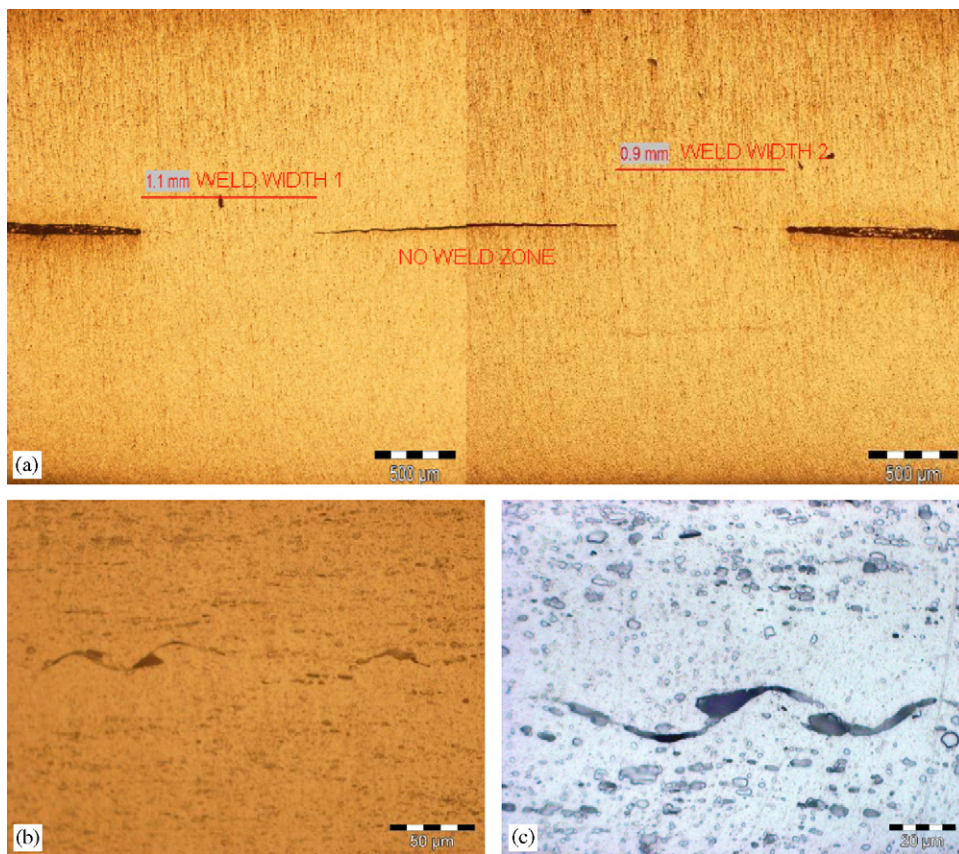


Fig. 15. Rectangular coil: effect of energy on weld width, (a) energy = 5 kJ, voltage = 7.2 kV, standoff distance = 2.5 mm; (b) energy = 3.6 kJ, voltage = 6 kV, standoff distance = 2.5 mm, discontinuous wavy weld at 500 × magnification; (c) energy = 3.6 kJ, voltage = 6 kV, standoff distance = 2.5 mm, discontinuous wavy weld at 1000 × magnification.

than that of the rectangular coil) at the discharge energy of 5 kJ and 40 MPa (38% higher than that of the rectangular coil) at 3.6 kJ discharge energy.

#### 4.2.2. Weld width

4.2.2.1. Rectangular coil. The samples welded at different discharge energies were examined metallographically for weld widths. Fig. 15 shows the representative photograph of weld widths obtained at different values

of energy. The total weld width is the sum of the two weld widths obtained. The values of the percentage weld widths obtained with flat rectangular coil with variation in energy are summarized in a graph shown in Fig. 13(a). It is observed that the increase in energy increased the width of the weld. Fig. 15(a) shows the total weld width of 2 mm is obtained at 5 kJ. The discontinuous weld is obtained at discharge energy of 3.6 kJ. It shows a discontinuous wavy interface since the physical boundaries of the two sheets are retained as evident in Figs. 15(b) and (c). It is similar to the one observed in transition zone between weld and no-weld zones obtained at higher energy (5 kJ) as shown in Fig. 11. This occurs because at the lower values of energy the velocity of impact is not sufficient to create continuous weld. If the discharge energy is greater than 3.6 kJ the welds show continuity of the metal as seen in Fig. 15(a).

**4.2.2.2. Tapered coil.** The weld widths obtained with the tapered coil show similar trends as those obtained with the flat rectangular coil. It was observed that the increase in energy increased the width of the weld. Fig. 16 shows the representative photograph of the weld widths obtained with energy of 5 kJ. The values of the percentage weld widths with variation in energy are summarized in graph shown in Fig. 13(b). A total weld width of 1.3 mm was obtained with the energy of 5 kJ (Fig. 16), whereas, a weld width of 0.3 mm was obtained with the energy of 4 kJ.

### 4.3. Effect of standoff distance on the weld strength and width

Aluminum sheets kept at some standoff distance get accelerated due to the electromagnetic impulse. Sheets fly towards each other with a very high velocity. At some optimum value of standoff distance the sheets attain a maximum velocity and acquire corresponding high kinetic energy. When these two sheets collide with each other the kinetic energy gets transformed into impact energy. Due to jetting and squirting of oxides the weld takes place. If the standoff distance is varied on either side of its optimum value, both the velocity and in turn the kinetic energy acquired by the sheets get reduced, leading to reduction in the shearing strength and the width of the weld. For the lower values of standoff distance, collision takes place before sheets attain the maximum velocity, whereas, for higher values the velocity attained drops to a lower value at the time of collision. Therefore, maximum strength of the weld is achieved only at the optimum value of the standoff distance for a given set of other process parameters. The effect of standoff distance on the strength and width of the weld was investigated at constant discharge energy of 5 kJ.

#### 4.3.1. Weld strength

**4.3.1.1. Rectangular coil.** The dependency of the shearing strength on the standoff distance for welds made using a flat rectangular coil is shown in Fig. 17(a). It was observed that for welding 1 mm thick aluminum sheets,

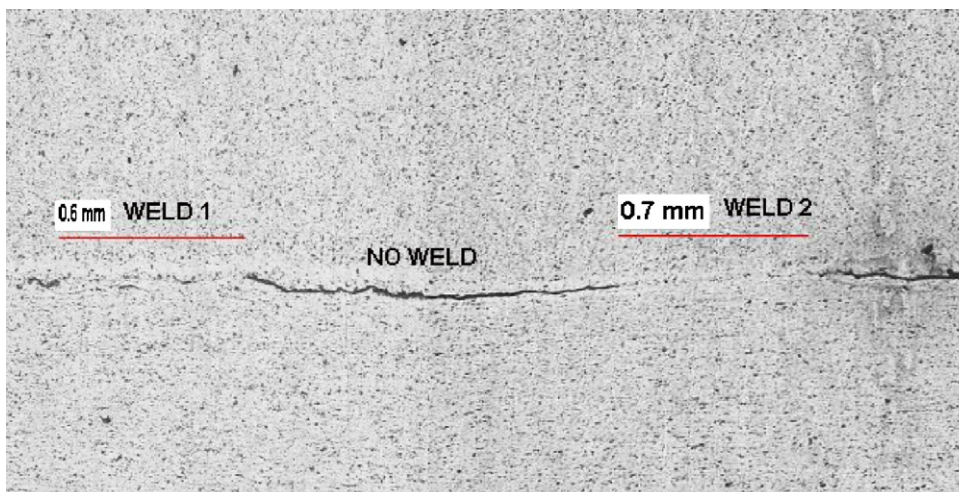


Fig. 16. Tapered coil: effect of energy on weld width, energy = 5 kJ, voltage = 7.2 kV, standoff distance = 2.5 mm.

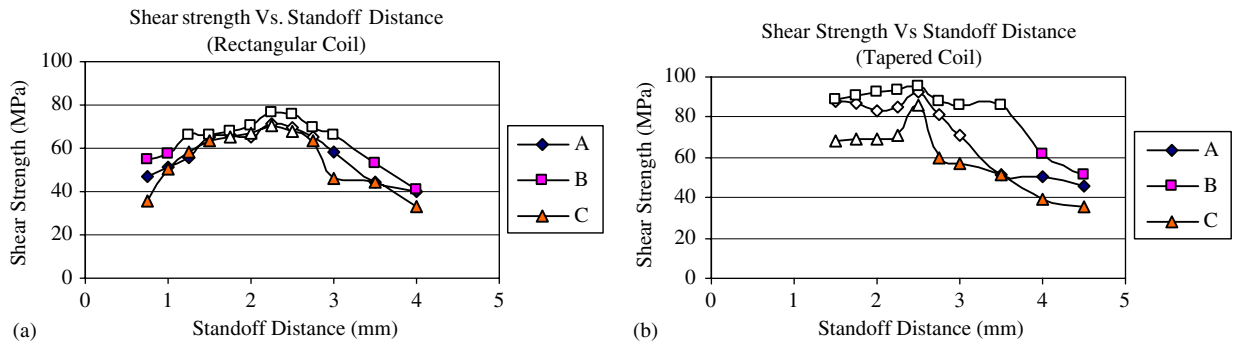


Fig. 17. (a) Rectangular coil: effect of standoff distance on shearing strength of weld at discharge energy of 5 kJ, (b) tapered coil: effect of standoff distance on shearing strength of weld at discharge energy of 5 kJ.

2.25 mm is the optimum standoff distance. When the standoff distance was varied on either sides from 2.25 mm the shearing strength decreased. The shearing strength obtained at 2.25 mm standoff distance was 77 MPa at discharge energy of 5 kJ. Similar to the results for variation in the energy, the test results for the variation in the standoff distance also showed that the 'B' pieces cut from the central part of the welds demonstrate higher shearing strength as compared to the 'A' and 'C' pieces cut from the edges of the welded samples.

**4.3.1.2. Tapered coil.** The effect of standoff distance on the shearing strength of the welds is shown in Fig. 17(b). The optimum standoff distance for the tapered coil was observed to be 2.5 mm. The shearing strength obtained at 2.5 mm standoff distance is in excess of 96 MPa. The value of the shearing strength decreased as the standoff distance was varied on either sides from its optimum value. The 'B' pieces cut from the central part of the welds show higher shearing strength as compared to the 'A' and 'C' pieces cut from the edges of the welded samples.

#### 4.3.2. Weld width

**4.3.2.1. Rectangular coil.** A study was carried out to investigate the effect of variation in standoff distance on the weld width. The weld width reduces as the standoff distance is varied from its optimum value. Fig. 18 shows the photographs of the weld widths achieved with three different standoff distances. The values of the percentage weld widths are summarized in a graph shown in Fig. 13(b). A weld width of 1.2 mm (Fig. 18(a)) is obtained at optimum standoff distance of 2.25 mm. When standoff distance is increased to 3.5 mm (Fig. 18(b)) the weld width reduces from 1.2 to 0.04 mm. When standoff distance is further increased to 4 mm a discontinuous weak bond is formed, as shown in Figs. 18(c) and (d). This occurs because at the higher values of standoff distance the velocity of impact is not sufficient to create continuous weld.

**4.3.2.2. Tapered coil.** Fig. 19 shows the photograph of the weld width obtained at standoff distances of 4.5 mm for tapered coil. The values of the percentage weld widths obtained with the tapered coil are summarized in the graph shown in Fig. 13(b).

## 5. Summary

In this work, a process of electromagnetic impact welding of aluminum sheets has been successfully established. The effects of variation in process parameters, viz. coil geometry, standoff distance and energy, on the welding process have been investigated. The following inferences can be drawn from the comprehensive experimental work:

1. Aluminum sheets of 1 mm thickness can be successfully welded by electromagnetic impact welding with capacitor discharge energy of 3.6 kJ.
2. The microstructure of the Al–Al welds obtained by EM welding shows two weld zones with complete metal continuity and one no-weld zone at center. The reasons for the no-weld zone are the possible entrapment of

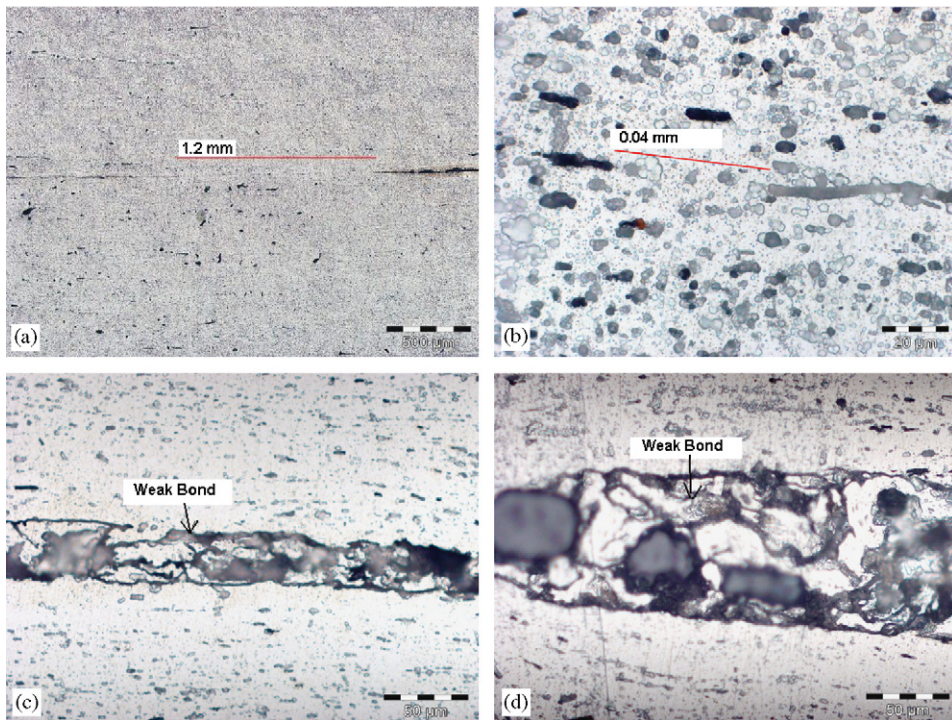


Fig. 18. Rectangular coil: effect of standoff distance on weld width, energy = 5 kJ, voltage = 7.2 kV, (a) standoff distance = 2.25 mm, weld width = 1.2 mm; (b) energy = 5 kJ, voltage = 7.2 kV, standoff distance = 3.5 mm, weld width = 0.04 mm; (c) energy = 5 kJ, voltage = 7.2 kV, standoff distance = 4 mm, discontinuous weld 1; (d) energy = 5 kJ, voltage = 7.2 kV, standoff distance = 4 mm, discontinuous weld 2.

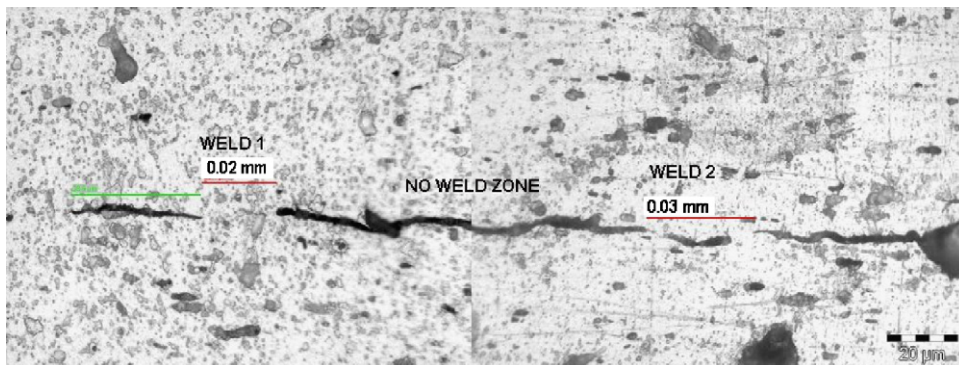


Fig. 19. Tapered coil: effect of standoff distance on weld width, energy = 5 kJ, voltage = 7.2 kV, standoff distance = 4.5 mm.

oxides, the rebound effect due to normally acting Lorentz force at the center, and the complex deformation state at the interface.

3. Reduction in the cross-section area of the coil (e.g. tapered coil) increases the current density leading to an increase in the shearing strength of the weld.
4. Increase in discharge energy for welding increases the magnetic field generated, and thus increases the shearing strength and the width of the weld for a given standoff distance. For the given setup, discontinuous wavy weld, similar to the one obtained at transition zone between weld and no-weld, was obtained at 3.6 kJ discharge energy. For energies higher than 3.6 kJ, continuous weld with metal continuity was obtained.

5. For given set of process parameters the standoff distance has one optimum value that gives the maximum shearing strength and width of the weld. Decrease or increase in the standoff distance from the optimum value results in reduction of the shearing strength and the width of the weld. The reason for this is that the sheets attain maximum velocity and the kinetic energy at some optimum value of standoff distance, below or above of which the sheets cannot fly with maximum velocity. For the lower values of standoff distance, collision takes place before sheets attain the maximum velocity, whereas, for higher values the velocity attained drops to a lower value at the time of collision.
6. The test pieces cut from the center of the welds exhibit greater shearing strength than the pieces cut from the edges. The reason for this behavior may be attributed to higher penetration of magnetic field at the center and change of current direction in the sheets at their edges. This weakens the magnetic field developed at the edges and hence the impulse acting on the sheets.

### Acknowledgements

Authors thank Dr. R.C. Sethi Head, APPD, BARC, and Dr. K.V. Nagesh, APPD, BARC, for kindly permitting the use of the experimental facility available at BARC. Authors also thank Mr. S.V. Desai, Mr. R.K. Rajawat, Mr. M.R. Kulkarni, Ms. Dolly Rani and Mr. Satendra Kumar from APPD, BARC for their valuable suggestions and help while conducting the experiments.

### References

- [1] Al-Hassani STS, Duncan JL, Johnson W. On the parameters of magnetic forming process. *J Mech Eng Sci* 1974;16(1):1–9.
- [2] Davis R, Austin ER. *Developments in high speed metal forming*. Industrial Press Inc.; 1970.
- [3] Plum MM, Maxwell Laboratories Inc. *Electromagnetic forming, metals handbook*, 9th ed. 14 ASM Metals Park, OH; 1996.
- [4] Balanethiram V. *Hyperplasticity: enhanced formability of sheet metals at high velocity*. PhD thesis, Material science and engineering. Columbus, OH, USA: The Ohio State University, 1996.
- [5] Padmanabhan M. *Wrinkling and springback in electromagnetic sheet metal forming and electromagnetic ring expansion*. MS thesis, Material science and engineering. Columbus, OH, USA: The Ohio State University, 1997.
- [6] Vohnout VJ. *A hybrid quasi-static/dynamic process for forming large sheet metal parts from aluminum alloys*. PhD thesis, Industrial welding and system engineering. Columbus, OH, USA: The Ohio State University; 1998.
- [7] Azab AEI, Garnich M, Kapoor A. Modeling of the electromagnetic forming of sheet metals: state-of-the-art and future needs. *J Mat Process Technol* 2003;142:744–54.
- [8] Mamalis AG, Manolakos DE, Kaldas AG, Koumoutsos AK. Electromagnetic forming and powder processing: trends and developments. *Appl Mech Rev* 2004;57(4):299–324.
- [9] Hwang WS, Lee JS, Kim NH, Sohn HS. Joining of copper tube to polyurethane tube by electromagnetic pulse forming. *J Mat Process Tech* 1993;37:83–93.
- [10] Powers HG. Bonding of aluminum by the capacitor discharge magnetic forming processes. *Weld J* 1967;46:507–10.
- [11] Marya M, Marya S. Interfacial microstructures and temperatures in aluminum—copper electromagnetic pulse welds. *Sci Technol Weld Joining* 2004;9(6):541–7.
- [12] Stern A, Aizenshtein M. Bonding zone formation in magnetic pulse welds. *Sci Technol Weld Joining* 2002;7(5):339–42.
- [13] Marya M, Marya S, Priem D. On the characteristics of electromagnetic welds between aluminum and other metals and alloys. *Weld World* 2005;49:74–84.
- [14] Shribman V, Stern A, Livshitz Y, Gafri O. Magnetic pulse welding produces high strength aluminum welds. *Weld J* 2002;81(4):33–7.
- [15] Kimchi M, Saho H, Cheng W, Krishnaswamy P. Magnetic pulse welding of aluminum tubes to steel bars. *Weld World* 2004;48:19–22.
- [16] Zhang P, Daehn G. Analysis of the electromagnetic impulse joining process with a field concentrator. In: Ghosh S, Jose M, Castro JM, Lee JK, editors. *Proceedings of the eighth international conference on numerical methods in industrial forming processes*, Columbus, OH, 2004. p. 1253–58.
- [17] Rajawat RK, Desai SV, Kulkarni MR, Rani D, Nagesh KV, Sethi RC. Electromagnetic forming—a technique with potential applications in accelerators. In: *Proceedings of APAC, Gyeongju, Korea, 2004*. p. 187–9.
- [18] Fenton GK, Daehn G. Modeling of electromagnetic formed sheet metal. *J Mater Process Tech* 1998;75:6–16.
- [19] Aizawa T, Okogawa K, Yoshizawa M, Henmi N. Impulse magnetic pressure seam welding of aluminium sheets. *Impact Eng Appl* 2001;827–32.
- [20] Aizawa T. Methods for electromagnetic pressure seam welding of Al/Fe sheets. *Weld Int* 2004;18(11):868–72.
- [21] Moon FC. *Magneto-Solid Mechanics*. Wiley-Interscience Publication; 1984.